HHS Public Access

Author manuscript

Biochim Biophys Acta. Author manuscript; available in PMC 2016 January 01.

Published in final edited form as:

Biochim Biophys Acta. 2015 January ; 1852(1): 34–46. doi:10.1016/j.bbadis.2014.11.006.

Novel Curcumin Analog C66 Prevents Diabetic Nephropathy via JNK Pathway with the Involvement of p300/CBP-mediated Histone Acetylation

Yangwei Wang[1,2], **Yonggang Wang**[2,3], **Manyu Luo**[1,2], **Hao Wu**[1,2], **Lili Kong**[1,2], **Ying Xin**[2,4], **Wenpeng Cui**[1,2], **Yunjie Zhao**[5], **Jingying Wang**[5], **Guang Liang**[5], **Lining Miao**[1,*], and **Lu Cai**[2,6,*]

[1]Department of Nephrology, Second Hospital of Jilin University, Changchun, China

[2]Kosair Children's Hospital Research Institute and Department of Pediatrics of University of Louisville, Louisville, KY, USA

[3]Cardiovascular Center, First Hospital of Jilin University, Changchun, China

[4]Key Laboratory of Pathobiology, Ministry of Education, Jilin University, Changchun, China

[5]Chemical Biology Research Center, School of Pharmaceutical Sciences, Wenzhou Medical University, Wenzhou, China

[6]Departments of Radiation Oncology and Pharmacology & Toxicology, University of Louisville, Louisville, KY, USA

Abstract

Glomerulosclerosis and interstitial fibrosis represent the key events in development of diabetic nephropathy (DN), with connective tissue growth factor (CTGF), plasminogen activator inhibitor-1 (PAI-1) and fibronectin 1 (FN-1) playing important roles in these pathogenic processes. To investigate whether the plant metabolite curcumin, which exerts epigenetic modulatory properties when applied as a pharmacologic agent, may prevent DN via inhibition of the JNK pathway and epigenetic histone acetylation, diabetic and age-matched non-diabetic control mice were administered a 3-month course of curcumin analogue (C66), c-Jun N-terminal kinase inhibitor (JNKi, sp600125), or vehicle alone. At treatment end, half of the mice were sacrificed for analysis and the other half were maintained without treatment for an additional 3 months. Renal JNK phosphorylation was found to be significantly increased in the vehicle-treated diabetic mice, but not the C66- and JNKi-treated diabetic mice, at both the 3-month and 6-month time points. C66 and JNKi treatment also significantly prevented diabetes-induced renal fibrosis and dysfunction. Diabetes-related increases in histone acetylation, histone acetyl transferases'

*Corresponding authors. Dr. Lining Miao, MD, PhD, Second Hospital of Jilin University, 218 Ziqiang Street, Changchun 130041, China; Tel/Fax: 86-431-88796520/86-431-88796975, miaolining55@163.com. Dr. Lu Cai, MD, PhD, Kosair Children's Hospital Research Institute at the University of Louisville, Louisville, KY 20202, USA; Tel/Fax: (502)852-2214, l0cai001@louisville.edu.

(HATs) activity, and the p300/CBP HAT expression were also significantly attenuated by C66 or JNKi treatment. Chromatin immunoprecipitation assays showed that C66 and JNKi treatments decreased H3-lysine9/14-acetylation (H3K9/14Ac) level and p300/CBP occupancy at the CTGF, PAI-1 and FN-1 gene promoters. Thus, C66 may significantly and persistently prevent renal injury and dysfunction in diabetic mice via down-regulation of diabetes-related JNK activation and consequent suppression of the diabetes-related increases in HAT activity, p300/CBP expression, and histone acetylation.

Keywords

diabetic nephropathy; fibrosis; JNK; p300/CBP; histone acetylation; curcumin

1. Introduction

Diabetic nephropathy (DN) is a common complication due to diabetes and the most common cause of end-stage renal disease [1]. The pathogenesis of DN involves genetic, environmental and hemodynamic changes. These changes may cause oxidative stress and inflammation, which leads to accumulation of extracellular matrix (ECM) proteins and renal glomerulosclerosis (fibrosis). Eventually glomerular dysfunction and renal failure will occur [2–4]. It is known that pro-fibrotic cytokines (e.g. connective tissue growth factor (CTGF), plasminogen activator inhibitor 1 (PAI-1), and fibrotic cytokines fibronectin 1 (FN-1)) play important roles in the development and progression of diabetic renal fibrosis [5–7]. Understanding the exact mechanisms is needed for developing novel therapeutic approaches to prevent renal fibrosis.

The c-Jun N-terminal kinase (JNK) pathway mediates important intracellular responses, such as cell growth and differentiation, and cell death [8]. JNK proteins belong to the mitogen activated protein kinase (MAPK) family. In the presence of oxidative stress and inflammation, the MAPK kinases, MKK4 and MKK7 activate JNK proteins via phosphorylation [9]. The JNK pathway has been implicated in the development of insulin resistance in obese and diabetic mice [10] and has been shown to be activated significantly in response to inflammatory cytokines and oxidative stress in diabetic or high glucose conditions [11, 12]. Furthermore, a previous study demonstrated that the JNK pathway was involved in the progression of diabetic renal fibrosis and the regulation of FN-1 accumulation in renal interstitial fibroblasts [13, 14]. In support of the theorized important role of JNK activation in DN, the JNK specific inhibitor, SP600125, was shown to significantly alleviate the pathogenesis of DN [15].

Histone acetylation may be another mechanism involved in the etiology of diabetes and the development of its complications [16]. Histone modification is a reversible dynamic process controlled by histone acetyl transferase (HAT) and histone deacetylase (HDAC). These processes regulate chromatin structure to facilitate or inhibit the transcription of genes [17]. p300/CREB-binding protein (CBP) is an important HAT in diabetes. For example, p300 was shown to be up-regulated and histone acetylation was shown to be increased in the retina and heart of diabetic animals [18]. Moreover, under high glucose conditions, p300 is

induced and histone acetylation is increased in endothelial cells, resulting in the regulation of vasoactive factors and ECM proteins [19]. Activation of the JNK pathway can also up-regulate p300 activity and histone acetylation, thereby increasing the transcription of correlative genes [20], making inhibition of p300 activity and histone acetylation a potential therapeutic target for DN.

Curcumin has several known pharmacological effects, including anti-inflammatory, anti-oxidative, and anti-fibrosis [21–24]. Administration of curcumin to diabetic animals effectively prevented high glucose- and diabetes-induced oxidative stress in the endothelial cells and heart [25]. A clinical trial has demonstrated that dietary curcumin significantly prevented the pathogenesis and progression of diabetes and significantly reduced diabetic complications through its anti-inflammatory effects [26]. In addition, the activation of the JNK pathway was down-regulated by curcumin, which protected the kidney and heart from diabetes-induced pathogenic changes [27]. Finally, curcumin specifically inhibits p300. After curcumin treatment, p300 activity and histone acetylation were decreased in monocytes grown in a high glucose environment, ultimately leading to a decrease in pro-inflammatory cytokines [28].

Despite great therapeutic potential, the clinical efficacy of curcumin is limited by its low bioavailability [26, 29]. Therefore, we developed a curcumin analogue, C66 [(2E,6E)-2,6-bis(2-(trifluoromethyl)benzylidene)cyclohexanone], which has the same efficacy at 50 – 200 fold lower doses as curcumin [30, 31]. We previously showed that C66 can significantly inhibit high glucose-induced MAPK phosphorylation and downstream inflammatory responses in murine macrophages [30]. In the current study, we investigated whether C66 is able to prevent DN via suppression of diabetes-induced JNK pathway activation, induction of p300/CBP HAT activity, and histone hyperacetylation in the kidney. To this end, we used the same samples from the animals that were used in a related study that was recently published [32].

2. Materials and methods

2.1. Animals

The samples used in this study are the same as in our recently published study [32]. Briefly, 8 – 10 week old C57BL/6J male mice (Jackson Laboratory, Bar Harbor, ME, USA) were housed in the University of Louisville Research Resources Center at 22°C with 12 h light/dark cycles, and given free access to standard rodent chow and tap water. All experimental procedures for the animal usage were in accordance with the Guide for the Care and Use of Laboratory Animals and were approved by the Institutional Animal Care and Use Committee of the University of Louisville.

The type 1 diabetes mouse model was induced with a single intraperitoneal injection of streptozotocin (STZ) (in sodium citrate, pH=4.5; Sigma-Aldrich, St. Louis, MO, USA) at 150 mg/kg; the aged-matched non-modeled mice (control) were given the same volume of sodium citrate buffer. Blood glucose was monitored on the 3rd day after injection, and hyperglycemia (blood glucose levels ≥ 250 mg/dL) was noted in the STZ-injected mice. Both control and diabetic mice were randomly divided into the following three groups (n=10

each): control group, C66 group, and JNKi (sp600125) group. These groups were treated by gavage with vehicle, C66 or JNKi (C66 and JNKi dissolved in 1% CMC-Na solution), respectively. All solutions were administered at 5 mg/kg, every other day for 3 months. In a previous study, the JNKi was administered at 30 mg/kg for short times [33], but we chose to administer it at a relatively low dose to avoid any potential toxic effects of accumulated doses of JNKi for the 3-month usage. At the end of the 3-month treatment, one set of both diabetic and control mice (n=4 or 5) from each group was sacrificed and labeled as the 3-month study cohort. Another set of both diabetic and control mice (n=4 or 5) from each group was aged for additional 3 months without further treatment and labeled as the 6-month study cohort.

2.2. Renal function measurement

Spot urine and serum samples were collected immediately before sacrifice. Commercial kits were used to measure urinary albumin (Bethyl Laboratories, Montgomery, TX, USA) and urinary and serum creatinine (BioAssay Systems, Hayward, CA, USA) concentrations. The urinary albumin-to-creatinine ratio (ACR) was calculated as [urine albumin (μg/mL)] divided by [urine creatinine (mg/dL)] and presented as relative to values calculated for the control group.

2.3. Histopathological and immunofluorescent staining

Kidney tissue was fixed overnight in 10% phosphate-buffered formalin, dehydrated in a graded alcohol series, cleared with xylene, embedded in paraffin, and sectioned to 5 μm thickness. To examine overall morphology, the paraffin sections were dewaxed for hematoxylin-eosin (H&E) staining, as previously described [34], or with Masson's trichrome, using the Sigma-Aldrich Trichrome Staining Kit. For immunofluorescent staining, the paraffin-embedded kidney sections were incubated with H3K9/14Ac primary antibody (1:2000; Cell Signaling Technology, Danvers, MA, USA), after which sections were washed with phosphate-buffered saline plus 0.1% Triton (PBS-T) (EM Science, Hawthorne, NY, USA) and incubated with FITC-conjugated IgG secondary antibody (1:200; Abcam, Cambridge, UK) for 1 h at room temperature. After a final PBS-T wash, the immunostained sections were counterstained with DAPI (Sigma–Aldrich) and assessed with imaging analysis software (NIS-Elements BR 3.0; Nikon, Tokyo, Japan) under a fluorescence microscope (Nikon).

2.4. RNA isolation and real-time polymerase chain reaction (PCR)

Total RNA was extracted and purified from kidney tissues using the Trizol Reagent (Invitrogen, Carlsbad, CA, USA) according to the manufacturer's protocol. The concentration and integrity of the isolated RNA was spectrophotometrically measured using the NanoDrop 1000 (Thermo Fisher Scientific, Wilmington, DE, USA). The RNA (1 μg) was used as template to generate cDNA by reverse transcription with the *Taq*Man Reverse Transcription Kit (Applied Biosystems Inc., Foster City, CA, USA). The real-time PCR amplification reactions were carried out in 20 μL reactions, as follows: 10 μL of *Taq*Man Universal PCR Master Mix (Promega, Madison, WI, USA), 1 μL of each primer, 3 μL of cDNA, and 6 μL double-deionized H_2O. The following primers were purchased from Life

Technologies Corporation (Carlsbad, CA, USA): p300 (Mm00625535_m1), CBP (Mm01342452_m1), FN-1 (Mm01256744_m1) and GAPDH (Mm99999915_g1). The reaction process was carried out in an ABI 7500 Real-Time PCR system (Applied Biosystems Inc.), using 40 amplification cycles in a two-step cycling procedure (denaturation at 95°C for 15 s; annealing at 60°C for 1 m). The comparative cycle time (Ct) method was used to determine fold-differences between samples, with the values normalized to the GAPDH endogenous reference and relative to a calibrator ($2^{-\Delta\Delta Ct}$).

2.5. Western blot assay

Unprocessed kidney tissues were mechanically homogenized in RIPA lysis buffer and centrifuged (12 000 rpm at 4°C) to remove cell debris. The total proteins (supernatant) were collected and assessed by the Bradford protein assay (Bio-Rad, Hercules, CA, USA) to measure the concentration before resolving by electrophoresis through a 10% SDS-PAGE gel (at 110 V) and electrotransferring to a 0.22 mm polyvinylidene difluoride membrane. Any non-specific binding sites on the transferred membrane were blocked by incubating in TBS containing 5% non-fat milk and 0.5% BSA for 1 h at room temperature. Specific protein detection was then carried out by incubating with the following primary antibodies overnight at 4°C: 1:1000 CTGF (sc-14939; Santa Cruz Biotechnology, Dallas, TX, USA), 1:5000 PAI-1 (612024; BD Bioscience, San Jose, CA, USA), 1:2000 H3K9/14Ac (9677s; Cell Signaling Technology), 1:1000 phosphorylated-JNK (9255s; Cell Signaling Technology), 1:1000 JNK (9252; Cell Signaling Technology), and 1:3000 β-actin (sc-1616; Santa Cruz Biotechnology). The membranes were then washed three times with TBS containing 0.1% Tween-20 and incubated with the appropriate horseradish peroxidase-conjugated secondary antibodies for 1 h at room temperature. Immunoreactive bands were visualized by the enhanced chemiluminescent substrate (Bio-Rad).

2.6. Histone acetyltransferase activity assay

HATs activity in kidney tissues was quantified using the colorimetric HATs Activity Assay Kit (Abcam) according to the manufacturer's protocol. Briefly, the nuclear extract was first isolated from renal tissues using a Nuclei Isolation Kit (Sigma-Aldrich) and 50 μg was then incubated with HAT substrates I and II and the NADH-generating enzyme (in the HAT assay buffer) at 37°C for 1 to 4 h, depending on the color development. The OD_{440nm} was read at different times in a microplate reader (Bio-Rad). Water was used as a negative control and control nuclear extracts provided by the manufacturer were used as the positive controls. HATs' activity was expressed as the relative OD_{440nm} value per microgram per minute.

2.7. Chromatin immunoprecipitation (CHIP) assay

The ChIP assay was carried out using the EpiQuik™ Tissue ChIP Kit (P-2003; Epigentek Group Inc., Farmingdale, NY, USA), following the manufacturer's instructions. Briefly, the assay wells were first coated with 2 μg of the specific antibody for a 90 min incubation at room temperature. The following antibodies were tested: H3K9/14Ac (9677s; Cell Signaling Technology), p300 (sc-585x; Santa Cruz Biotechnology), and CBP (7389s; Cell Signaling Technology). Negative and positive controls were established with 1 μL of normal mouse IgG and anti-RNA polymerase II, respectively. Meanwhile, 70 μg of kidney tissues were cut

into small pieces and cross-linked with 1% formaldehyde in PBS at room temperature for 15 to 20 min. Glycine solution (1.25 M) was added to stop the reaction. Tissue pieces were disaggregated and the nuclei were isolated, after which the DNA was sheared by sonication using a Branson Digital Sonifier (S-450-D with micro-tip probe; Emerson Industrial, St. Louis, MO, USA) with five pulses of 20 s each separated by 35 s rest intervals. After centrifugation, 5 μL of the diluted supernatants were removed for use as input DNA. The other 100 μL was transferred to the antibody-coated wells and incubated at room temperature for 90 min. ChIP-enriched DNA samples were collected and purified. ChIP-enriched DNA and input DNA were analyzed by real-time PCR with the following primers: CTGF forward 5'-GAGCTGAGTACATCATCTCAC-3', reverse 5'-GGACATTCAAGACATTCACAG-3'; PAI-1 forward 5'-CACCAGGAGAGTCTGGCCCCATGT-3', reverse 5'-ACTTCAAGTCCTTTCCTCCTCCCT-3'; FN-1 forward 5'-GGAGTCGGACCGGACCC-3', and reverse 5'-GTTGAGCCCCAAGAGCAGAG-3'. Data were analyzed relative to a calibrator ($2^{-\Delta\Delta Ct}$) and normalized to input samples.

2.8. Statistical analysis

Data were collected from four to five animals for each group and presented as mean ± SD. ImageQuant 5.2 was used to analyze the western blotting results. OriginLab 7.5 data analysis and graphing software were used to carry out comparisons between groups by one-way ANOVA, followed by a Tukey's *post hoc* test. Statistical significance was considered if $P < 0.05$.

3. Results

3.1. C66 prevented diabetes-induced renal dysfunction and hypertrophy

Body weight and blood glucose were recorded from 7 to 67 days after STZ administration. We showed previously [32] that the body weight and heart weight in the diabetic mice (DM) and DM + C66 was reduced. The C66 treatment also did not affect the blood glucose profile of diabetic mice.

Spot urinary albumin and urinary creatinine were measured. The ACR was calculated as an index of renal function. At 3-months of treatment (Fig. 1A), the ACR increased significantly in DM relative to control. After treatment with C66 for 3 months, the ACR was slightly ($P >0.05$) reduced. However, after treatment with JNKi for 3 months, the ACR was significantly reduced ($P <0.05$). After 6 months, the ACR was significantly ($P <0.05$) increased in DM compared to control mice (Fig. 1B). The diabetic effect was significantly ($P <0.05$) reduced by the 3-month C66 treatment, and only slightly reduced by the 3-month JNKi treatment. It is known that serum creatinine levels often increase at the late stages of DN. We observed significantly ($P <0.05$) increased serum creatinine levels in DM that was significantly ($P <0.05$) reduced by treatment with either C66 or JNKi (Fig. 1C).

Kidney weights were evaluated by examining the kidney weight to tibia length ratio. There was no significant difference for the ratio of kidney weight to tibia length among groups after 3 months (Fig. 1D). After 6 months, (Fig. 1E) the kidney weight to tibia ratio was

significantly (P <0.05) increased in the DM group, but not DM + C66 and DM + JNKi groups. This suggests that the diabetic mice may have renal hypertrophy that is attenuated by C66 or JNKi treatment. Taken together, these data showed that C66 and JNKi act similarly to prevent the diabetic renal effect

3.2. C66 down-regulated diabetes-related activation of JNK after 3 months of treatment, but the affect was not sustained after treatment stopped for 3 months

We next determined whether C66 has a direct effect on JNK activation under normal and diabetic conditions. Western blotting demonstrated that phosphorylated JNK protein level was significantly (P <0.05) increased in the kidneys of the DM group compared to the control group after 3 months and 6 months (Fig. 2A and B). Treatment of DM with either C66 or JNKi significantly decreased diabetic activation of JNK (the ratio of p-JNK/JNK), which was observed after 3 months but not 6 months (Fig. 2A and B). This finding suggests that C66 can significantly inhibit diabetic activation of JNK after treatment but does not maintain this effect once treatment was ceased. The phosphorylation level of c-jun, a downstream target of JNK, was measured to confirm the inhibitory effect of C66 on phosphorylated JNK. As expected, treatment with either C66 or JNKi in DM significantly (P <0.05) decreased phosphorylation c-jun protein levels (Fig. 2C). These findings suggest that C66 can suppress the diabetic activation of JNK.

3.3. C66 decreased diabetes-induced renal structural changes

Since JNKi can prevent diabetes-induced histological and biochemical changes, we determined the histological changes after C66 treatment. Renal tissue staining with H&E (Fig. 3A) and Masson's trichrome (Fig. 3B) revealed that diabetes induced a progressive increase in mesangial cells and glomerular enlargement (Fig. 3A, B, C, E), which was accompanied by progression of renal fibrosis, the latter being evidenced by increased ECM with Masson's trichrome (blue) staining (Fig. 3B, D, F). Both the C66 and JNKi treatments for 3 months significantly attenuated the diabetes-induced glomerular enlargement and renal fibrosis.

The development of diabetes-induced renal fibrosis was further confirmed by examination of a few key profibrotic cytokines, such as CTGF and PAI-1, by western blotting and real-time PCR. As shown in Figure 4, the expression of CTGF and PAI-1 was significantly increased in the kidneys of the DM mice, but not in the DM + C66 nor the DM + JNKi mice at either the 3-month (Fig. 4 A, B, G, H) or 6-month (Fig. 4 C, D, I, J) time point. When real-time PCR was used to examine the mRNA expression of FN-1 in the kidney (Fig. 4 E, F) it was found that administration of C66 or JNKi significantly prevented the diabetes-related up-regulation of renal FN-1 mRNA expression at both the 3-month and 6-month time point.

3.4. C66 prevented diabetic up-regulation of renal histone acetylation through down-regulation of p300/CBP expression and HATs' activity

The above results showed that, similar to the JNKi treatment, the 3-month C66 treatment of DM animals significantly prevented diabetes-related activation of renal JNK at the end of treatment, but the effect did not last for the 3 months following the termination of treatment

(Fig. 2). In contrast, both the C66 and JNKi 3-month treatments significantly prevented diabetes-induced renal dysfunction (Fig. 1) as well as the related histopathological changes, but these effects persisted out to 3 months after the treatments had been terminated. Diabetes itself causes progressive biochemical and cellular changes in various organs, a phenomenon known as the “metabolic memory effect” that involves epigenetic mechanisms [35]. The persistent prevention of diabetes-induced renal dysfunction and pathological changes provided by C66 and JNKi may also be related to epigenetic modulations. Since curcumin is a HAT inhibitor and can prevent p300/CBP activation, we tested whether C66 can prevent diabetes-related histone hyperacetylation through down-regulation of the expression and activation of HATs in the kidney. The locations of acetylated histone H3K9/14Ac in the kidney tissues were assessed by western blotting (Fig. 5A, B) and immunofluorescent staining (Fig. 5C). The DM mice showed significantly and progressively increased expression of H3K9/14Ac, as compared with age-matched controls, at both the 3-month and 6-month time points; however, the DM mice treated with C66 or JNKi for 3 months showed significant attenuation of the diabetes-related increase in the expression of H3K9/14Ac levels (Fig. 5A, 3 month study), which persisted through the 3 months after the end of treatment (Fig. 5B, 6 month study). Moreover, the detected expression of H3K9/14Ac was predominantly localized to the nuclei of both glomerular cells and renal tubular cells (Fig. 5C).

To test whether C66 prevented the renal expression and activity of HATs under the diabetic condition, real-time PCR was carried out to measure the mRNA expression of p300 (Fig. 6 A, B) and CBP (Fig. 6 C, D) in the kidney tissues and a colorimetric HAT activity assay was performed to measure the HAT activity (Fig. 6E,F). The DM mice showed significantly increased expression and activity of HAT, as compared with controls, at the 3-month time point, which persisted (without significant change) to the 6-month time point; however, treatment with either C66 or JNKi for 3 months significantly prevented the diabetes-related up-regulation of HAT expression and activity, and these effects lasted through the additional 3 months without treatment.

3.5. C66 prevented the diabetes-related increase in H3K9/14Ac level and p300/CBP occupancy on the promoters of CTGF, PAI-1, and FN-1 gene

The results described above demonstrated that C66 can suppress both total expression of H3K9/14Ac level and p300/CBP expression as well as the activity in kidneys of DM mice, suggesting a functional relationship between histone acetylation and fibrosis. Investigation of this potential pathogenic process by CHIP assay, using the H3K9/14Ac antibody to examine the H3K9/14Ac levels on the gene promoters of CTGF (Fig. 7A), PAI-1 (Fig. 7B) and FN-1 (Fig. 7C) in the kidney, showed that the DM mice had significantly increased levels for each, and that these levels were similar for the C66- and JNKi-treated DM mice.

The excessive histone acetylation at the CTGF, PAI-1 and FN-1 promoters in DM mice suggested an association with p300/CBP activation, which may be demonstrated by their occupancy at these genes’ promoters and indicate that C66 decreases the levels of histone acetylation at these promoters by suppressing the recruitment of CBP and p300. CHIP assay showed that the CTGF, PAI-1 and FN-1 gene promoter occupancy by CBP (Fig. 7D, E, F)

and p300 (Fig. 7G, H, I) was significantly increased in DM kidneys. Both C66 and JNKi treatment significantly prevented the diabetes-related increased promoter occupancy of p300 and CBP for CTGF (Fig. 7D, G) and PAI-1 (Fig. 7E, H), and this effect lasted through the additional 3 months of study following treatment termination. However, these C66- and JNKi-mediated preventive effects were very moderate for the diabetes-related p300 and CBP occupancy at the FN-1 promoter (Fig. 7F, I).

4. Discussion

In the present study, we demonstrated for the first time that C66, a novel curcumin analogue, can prevent diabetes-induced renal fibrosis, and the subsequent renal dysfunction, in STZ-induced diabetic mice by down-regulating the p300/CBP HAT expression and total HAT activation via suppression of JNK activation; this process is summarized in Figure 8.

The “metabolic memory” phenomenon, in which a previous exposure to hyperglycemia is associated with progression of diabetic vascular complications despite achievement of good glycemic control [35], may involve epigenetic modulation of chromatin [36–38]. As described in the introduction, accumulation of ECM and development of renal fibrosis can cause DN, and profibrotic cytokines (such as CTGF, PAI-1 and FN-1) play key roles in the progression of renal fibrosis to DN [3, 4]. In the present study, DM mice were observed to have significantly increased ACR and serum creatinine level at 3 and 6 months after the disease model was established, with H&E and Masson’s Trichrome staining showing renal pathological changes corresponding to the disease-related aberrations. In addition, these changes were found to be associated with significant increases in the expression of the fibrous cytokines, CTGF, PAI-1 and FN-1, in the diabetic kidney.

Histone acetylation is an important post-transcriptional modification of histones that leads to the recruitment of protein complexes/transcription factors essential for gene expression and its proper regulation. The p300/CBP complex has been extensively studied and characterized as an important HAT subtype for gene expression in general [39]. Recent studies have indicated that both the p300/CBP complex and histone acetylation modifications contribute to the development and persistence of diabetes and its complications. In particular, experiments using cultured monocytes showed that exposure to high glucose (hyperglycemic) conditions led to activation of CBP and increased histone H3 acetylation, culminating in up-regulated expression of genes with inflammation-related functions [40]. Results from related *in vivo* studies confirmed that the increased histone acetylation can lead to inflammatory gene transcription under diabetic conditions [40]. Moreover, data from a clinical trial suggested that elevated acetylated histone levels play an important role in both vascular injury and remodeling in Type 1 diabetes [41]. Similar to these collective findings, our study of the STZ-induced diabetes mouse model showed that the diabetic condition was associated with significant increases in total HAT activity and H3K9/14Ac level. Treating these diabetic mice with C66 led to significant decreases in the diabetes-related elevations in p300/CBP occupancy in the promoters of the CTGF, PAI-1 and FN-1, which ultimately led to decreased H3K9/14Ac level and CTGF, PAI-1 and FN-1 gene expression. Therefore, the renal protective property of C66 in diabetes may involve its ability to suppress HAT activity.

As a p300 inhibitor, curcumin can prevent p300-mediated HAT events. In cardiac myocytes, curcumin has been shown to down-regulate gene expression reducing histone acetylation [42]. In a previous study of diabetes, curcumin was shown to prevent high glucose that was otherwise induced by p300 mRNA up-regulation and protein production that increases acetylation levels in endothelial cells [19]. Similarly, in the present study we demonstrated that the curcumin analogue, C66, effectively protected against pathogenic events in diabetes by decreasing the diabetes-related enhancement of p300/CBP mRNA expression, HATs' activation, and H3K9/14Ac levels in the kidney. Moreover, immunofluorescence staining showed increased H3K9/14Ac in the diabetic kidney, the expression of which was localized to the nuclei of both glomerular cells and renal tubular cells. To further understand the regulation of histone acetylation mediated by cytokines related to renal fibrosis, specifically CTGF, PAI-1 and FN-1, we investigated the levels of H3K9/14Ac and p300/CBP occupancy at the promoters of these genes after 6 months of the diabetic model being established. While the diabetic condition was associated with increased level of H3K9/14Ac and p300/CBP occupancy at these genes' promoters in the kidney, the treatment with C66 and JNKi resolved these aberrations.

Another important and novel finding of the present study is that C66 renal protection is mediated by inactivation of JNK. It has been previously shown that the JNK pathway can be activated by high glucose, with the subsequent up-regulated expression of fibrosis cytokines and promotion of renal fibrosis [14]. Since our previous study also showed the relatedness of JNK inactivation and C66 prevention of diabetic renal damage, a group of diabetic mice treated with JNKi was included in the present study to confirm that JNK activation is a pivotal mediator of diabetic renal fibrosis and the eventual development of DN. Our studies of these JNKi-treated DM mice provided similar results to those observed in the C66-treated DM mice. Activation of the JNK pathway can regulate recruitment of p300 and enhancement of histones H3 and H4 acetylation [43]. Accordingly, we concluded that the C66 treatment of diabetic mice down-regulates diabetes-increased p300/CBP expression and HATs activation via inactivation of JNK, and the subsequent histone hyperacetylation causes specific increases in the accumulation of p300/CBP at the promoters of CTGF, PAI-1 and FN-1 genes, as presented in Figure 8.

Thus, we report here for the first time that C66 can act as a strong preventive agent against diabetes-induced renal fibrosis and renal injury in the STZ-induced mouse model of diabetes though down-regulation of JNK pathway activation. More importantly, investigations of these mice at 3 months after the treatment had been terminated showed that neither the C66 treatment nor the JNKi treatment could suppress the diabetes-related stimulation of JNK phosphorylation. However, the C66- and JNKi-mediated prevention of diabetes-induced renal dysfunction and structure changes and increased expression of fibrosis cytokines persisted through 3 additional months after the treatments had been terminated. Diabetes-related activation of the JNK pathway in the kidney via epigenetic mechanisms, and the subsequent up-regulation of renal fibrotic signaling are prevented by C66 treatment, in this study by a 3-month treatment course. The persistence of these C66 protective effects may be related to the ability of C66 to suppress p300/CBP activation via long-term epigenetic modifications, which may affect the "metabolic memory" that may underlie the diabetic condition [44, 45]. Therefore, the present study provides the first evidence to support early

application of C66 to prevent diabetes-induced renal early activation of JNK and the consequent p300/CBP expression and HAT activation via epigenetic mechanisms; in essence, C66 may represent a therapeutic approach to provide a “protective memory”, facilitating sustained renal protection from diabetes even 3 months after the end of treatment.

In summary, our study provides extensive evidence that diabetes activates the JNK pathway, which in turn induces an epigenetic mechanism via stimulation of p300/CBP expression and HATs’ activation, subsequently increasing the transcription of fibrotic genes, such as CTGF, PAI-1 and FN-1. Ultimately, these molecular events promote renal fibrosis and kidney dysfunction. Moreover, C66 can provide an enduring renal protective effect through its down-regulation of the JNK pathway and induction of epigenetic changes, providing a “renal protective memory”. Another important insight provided by this study is that the JNK pathway and HATs, as well as histone acetylation, may represent a novel therapeutic strategy by which to combat the development of diabetic complications; considering that C66 is a curcumin analogue, with significant efficacy at lower doses than the plant compound curcumin, C66 holds particular promise for clinical application to diabetic patients, especially for prevention of DN. Future studies are warranted to study the efficacy and safety of this potential therapeutic agent in humans.

There are some limitations inherent to the design of the present study, which must be considered when interpreting our findings. First, a high dose of STZ (used to establish our diabetic mouse model) may be cytotoxic to kidneys, due to its tubular toxicity, which may occlude distinguishing DN-related neuropathy from STZ-induced nephropathy [46, 47]. Even though we used a high dose of STZ (delivered as a single intraperitoneal injection of 150 mg/kg) to establish the diabetic model, our investigations were carried out at 3 and 6 months after the STZ administration; this strategy minimized the potential role of tubular toxicity, but did not eliminate it. Establishing the model by using a repeated injection of low dose STZ (50 mg/kg/day × 5 days) would have been more appropriate [48], and future studies should consider this modeling approach. Second, the STZ-induced diabetes model was established in C57BL/6J mice in the present study. It is important to note that, although C57BL/6J mice are valuable tools for studying diet-induced obesity, hyperglycemia and hyperinsulinemia, these mice exhibit very limited features of DN [49]. Therefore, the use of a mouse strain with more DN susceptibility, such as 129 SvEv mice [50], may be preferable and may reveal more information regarding the C66- and/or JNK-mediated prevention of the early and late features of DN. In addition, although we have clearly indicated the predominant role of the JNK pathway in the development of DN, and its prevention by C66 and JNKi, it remains unknown whether other pathways are affected by these drugs.

Acknowledgments

This work was supported, in part, by grants from the National Science Foundation of China (No. 81170669, to LM; Nos. 81261120560 and 81200572, to GL; No. 81200525, to WC) and the United States National Institute of Health (No. 1R01DK 091338-01A1, to LC).

References

1. Kanwar YS, Sun L, Xie P, Liu FY, Chen S. A glimpse of various pathogenetic mechanisms of diabetic nephropathy. Annu Rev Pathol. 2011; 6:395–423. [PubMed: 21261520]
2. Wolf G. New insights into the pathophysiology of diabetic nephropathy: from haemodynamics to molecular pathology. Eur J Clin Invest. 2004; 34:785–796. [PubMed: 15606719]
3. Schena FP, Gesualdo L. Pathogenetic mechanisms of diabetic nephropathy. J Am Soc Nephrol. 2005; 16(Suppl 1):S30–S33. [PubMed: 15938030]
4. Qian Y, Feldman E, Pennathur S, Kretzler M, Brosius FC 3rd. From fibrosis to sclerosis: mechanisms of glomerulosclerosis in diabetic nephropathy. Diabetes. 2008; 57:1439–1445. [PubMed: 18511444]
5. Hishikawa K, Oemar BS, Nakaki T. Static pressure regulates connective tissue growth factor expression in human mesangial cells. J Biol Chem. 2001; 276:16797–16803. [PubMed: 11278731]
6. Malgorzewicz S, Skrzypczak-Jankun E, Jankun J. Plasminogen activator inhibitor-1 in kidney pathology (Review). Int J Mol Med. 2013; 31:503–510. [PubMed: 23314920]
7. Li Y, Chen Q, Liu FY, Peng YM, Wang S, Li J, Li J, Duan SB, Sun L, Ling GH, Luo JH. Norcantharidin inhibits the expression of extracellular matrix and TGF-beta1 in HK-2 cells induced by high glucose independent of calcineurin signal pathway. Lab Invest. 2011; 91:1706–1716. [PubMed: 21931301]
8. Johnson GL, Lapadat R. Mitogen-activated protein kinase pathways mediated by ERK, JNK, and p38 protein kinases. Science. 2002; 298:1911–1912. [PubMed: 12471242]
9. Czaja MJ. JNK regulation of hepatic manifestations of the metabolic syndrome. Trends Endocrinol Metab. 2010; 21:707–713. [PubMed: 20888782]
10. Hirosumi J, Tuncman G, Chang L, Gorgun CZ, Uysal KT, Maeda K, Karin M, Hotamisligil GS. A central role for JNK in obesity and insulin resistance. Nature. 2002; 420:333–336. [PubMed: 12447443]
11. Zhou L, Xue H, Wang Z, Ni J, Yao T, Huang Y, Yu C, Lu L. Angiotensin-(1–7) attenuates high glucose-induced proximal tubular epithelial-to-mesenchymal transition via inhibiting ERK1/2 and p38 phosphorylation. Life Sci. 2012; 90:454–462. [PubMed: 22285598]
12. Waeber G, Delplanque J, Bonny C, Mooser V, Steinmann M, Widmann C, Maillard A, Miklossy J, Dina C, Hani EH, Vionnet N, Nicod P, Boutin P, Froguel P. The gene MAPK8IP1, encoding islet-brain-1, is a candidate for type 2 diabetes. Nat Genet. 2000; 24:291–295. [PubMed: 10700186]
13. Watanabe N, Shikata K, Shikata Y, Sarai K, Omori K, Kodera R, Sato C, Wada J, Makino H. Involvement of MAPKs in ICAM-1 expression in glomerular endothelial cells in diabetic nephropathy. Acta Med Okayama. 2011; 65:247–257. [PubMed: 21860531]
14. Suzuki H, Uchida K, Nitta K, Nihei H. Role of mitogen-activated protein kinase in the regulation of transforming growth factor-beta-induced fibronectin accumulation in cultured renal interstitial fibroblasts. Clin Exp Nephrol. 2004; 8:188–195. [PubMed: 15480895]
15. Huang A, Yang YM, Yan C, Kaley G, Hintze TH, Sun D. Altered MAPK signaling in progressive deterioration of endothelial function in diabetic mice. Diabetes. 2012; 61:3181–3188. [PubMed: 22933112]
16. Jayaraman S. Epigenetics of autoimmune diabetes. Epigenomics. 2011; 3:639–648. [PubMed: 22126251]
17. Strahl BD, Allis CD. The language of covalent histone modifications. Nature. 2000; 403:41–45. [PubMed: 10638745]
18. Kaur H, Chen S, Xin X, Chiu J, Khan ZA, Chakrabarti S. Diabetes-induced extracellular matrix protein expression is mediated by transcription coactivator p300. Diabetes. 2006; 55:3104–3111. [PubMed: 17065349]
19. Chen S, Feng B, George B, Chakrabarti R, Chen M, Chakrabarti S. Transcriptional coactivator p300 regulates glucose-induced gene expression in endothelial cells. Am J Physiol Endocrinol Metab. 2010; 298:E127–E137. [PubMed: 19903865]
20. Luo SF, Lin CC, Chen HC, Lin WN, Lee IT, Lee CW, Hsiao LD, Yang CM. Involvement of MAPKs, NF-kappaB and p300 co-activator in IL-1beta-induced cytosolic phospholipase A2

expression in canine tracheal smooth muscle cells. Toxicol Appl Pharmacol. 2008; 232:396–407. [PubMed: 18708082]

21. Babu PS, Srinivasan K. Hypolipidemic action of curcumin, the active principle of turmeric (Curcuma longa) in streptozotocin induced diabetic rats. Mol Cell Biochem. 1997; 166:169–175. [PubMed: 9046034]
22. Hanai H, Sugimoto K. Curcumin has bright prospects for the treatment of inflammatory bowel disease. Curr Pharm Des. 2009; 15:2087–2094. [PubMed: 19519446]
23. Hasan ST, Zingg JM, Kwan P, Noble T, Smith D, Meydani M. Curcumin modulation of high fat diet-induced atherosclerosis and steatohepatosis in LDL receptor deficient mice. Atherosclerosis. 2014; 232:40–51. [PubMed: 24401215]
24. Gupta SC, Patchva S, Aggarwal BB. Therapeutic roles of curcumin: lessons learned from clinical trials. AAPS J. 2013; 15:195–218. [PubMed: 23143785]
25. Farhangkhoee H, Khan ZA, Chen S, Chakrabarti S. Differential effects of curcumin on vasoactive factors in the diabetic rat heart. Nutr Metab (Lond). 2006; 3:27. [PubMed: 16848894]
26. Chuengsamarn S, Rattanamongkolgul S, Luechapudiporn R, Phisalaphong C, Jirawatnotai S. Curcumin extract for prevention of type 2 diabetes. Diabetes Care. 2012; 35:2121–2127. [PubMed: 22773702]
27. Pan Y, Zhu G, Wang Y, Cai L, Cai Y, Hu J, Li Y, Yan Y, Wang Z, Li X, Wei T, Liang G. Attenuation of high-glucose-induced inflammatory response by a novel curcumin derivative B06 contributes to its protection from diabetic pathogenic changes in rat kidney and heart. J Nutr Biochem. 2013; 24:146–155. [PubMed: 22819547]
28. Yun JM, Jialal I, Devaraj S. Epigenetic regulation of high glucose-induced proinflammatory cytokine production in monocytes by curcumin. J Nutr Biochem. 2011; 22:450–458. [PubMed: 20655188]
29. Dhillon N, Aggarwal BB, Newman RA, Wolff RA, Kunnumakkara AB, Abbruzzese JL, Ng CS, Badmaev V, Kurzrock R. Phase II trial of curcumin in patients with advanced pancreatic cancer. Clin Cancer Res. 2008; 14:4491–4499. [PubMed: 18628464]
30. Pan Y, Wang Y, Cai L, Cai Y, Hu J, Yu C, Li J, Feng Z, Yang S, Li X, Liang G. Inhibition of high glucose-induced inflammatory response and macrophage infiltration by a novel curcumin derivative prevents renal injury in diabetic rats. Br J Pharmacol. 2012; 166:1169–1182. [PubMed: 22242942]
31. Pan Y, Zhang X, Wang Y, Cai L, Ren L, Tang L, Wang J, Zhao Y, Wang Y, Liu Q, Li X, Liang G. Targeting JNK by a new curcumin analog to inhibit NF-kB-mediated expression of cell adhesion molecules attenuates renal macrophage infiltration and injury in diabetic mice. PLoS One. 2013; 8:e79084. [PubMed: 24260158]
32. Pan Y, Wang Y, Zhao Y, Peng K, Li W, Wang Y, Zhang J, Zhou S, Liu Q, Li X, Cai L, Liang G. Inhibition of JNK phosphorylation by a novel curcumin analog prevents high glucose-induced inflammation and apoptosis in cardiomyocytes and the development of diabetic cardiomyopathy. Diabetes. 2014; 63:3497–3511. [PubMed: 24848068]
33. Ramirez-Alcantara V, LoGuidice A, Boelsterli UA. Protection from diclofenac-induced small intestinal injury by the JNK inhibitor SP600125 in a mouse model of NSAID-associated enteropathy. Am J Physiol Gastrointest Liver Physiol. 2009; 297:G990–G998. [PubMed: 20501447]
34. Miao X, Bai Y, Sun W, Cui W, Xin Y, Wang Y, Tan Y, Miao L, Fu Y, Su G, Cai L. Sulforaphane prevention of diabetes-induced aortic damage was associated with the up-regulation of Nrf2 and its down-stream antioxidants. Nutr Metab (Lond). 2012; 9:84. [PubMed: 22978402]
35. White NH, Sun W, Cleary PA, Danis RP, Davis MD, Hainsworth DP, Hubbard LD, Lachin JM, Nathan DM. Prolonged effect of intensive therapy on the risk of retinopathy complications in patients with type 1 diabetes mellitus: 10 years after the Diabetes Control and Complications Trial. Arch Ophthalmol. 2008; 126:1707–1715. [PubMed: 19064853]
36. Villeneuve LM, Reddy MA, Lanting LL, Wang M, Meng L, Natarajan R. Epigenetic histone H3 lysine 9 methylation in metabolic memory and inflammatory phenotype of vascular smooth muscle cells in diabetes. Proc Natl Acad Sci U S A. 2008; 105:9047–9052. [PubMed: 18579779]

37. Zhong Q, Kowluru RA. Role of histone acetylation in the development of diabetic retinopathy and the metabolic memory phenomenon. J Cell Biochem. 2010; 110:1306–1313. [PubMed: 20564224]
38. Miao F, Chen Z, Genuth S, Paterson A, Zhang L, Wu X, Li S, Cleary P, Riggs A, Harlan D, Lorenzi G, Kolterman O, Sun W, Lachin J, Natarajan R. Evaluating the Role of Epigenetic histone modifications in the Metabolic Memory of Type 1 Diabetes. Diabetes. 2014; 63:1748–1762. [PubMed: 24458354]
39. Roth SY, Denu JM, Allis CD. Histone acetyltransferases. Annu Rev Biochem. 2001; 70:81–120. [PubMed: 11395403]
40. Miao F, Gonzalo IG, Lanting L, Natarajan R. In vivo chromatin remodeling events leading to inflammatory gene transcription under diabetic conditions. J Biol Chem. 2004; 279:18091–18097. [PubMed: 14976218]
41. Chen SS, Jenkins AJ, Majewski H. Elevated plasma prostaglandins and acetylated histone in monocytes in Type 1 diabetes patients. Diabet Med. 2009; 26:182–186. [PubMed: 19236624]
42. Sun H, Yang X, Zhu J, Lv T, Chen Y, Chen G, Zhong L, Li Y, Huang X, Huang G, Tian J. Inhibition of p300-HAT results in a reduced histone acetylation and down-regulation of gene expression in cardiac myocytes. Life Sci. 2010; 87:707–714. [PubMed: 21034749]
43. Tsai SY, Huang YL, Yang WH, Tang CH. Hepatocyte growth factor-induced BMP-2 expression is mediated by c-Met receptor, FAK, JNK, Runx2, and p300 pathways in human osteoblasts. Int Immunopharmacol. 2012; 13:156–162. [PubMed: 22504529]
44. Karukurichi KR, Wang L, Uzasci L, Manlandro CM, Wang Q, Cole PA. Analysis of p300/CBP histone acetyltransferase regulation using circular permutation and semisynthesis. J Am Chem Soc. 2010; 132:1222–1223. [PubMed: 20063892]
45. Villeneuve LM, Reddy MA, Natarajan R. Epigenetics: deciphering its role in diabetes and its chronic complications. Clin Exp Pharmacol Physiol. 2011; 38:451–459. [PubMed: 21309809]
46. Brouwers B, Pruniau VP, Cauwelier EJ, Schuit F, Lerut E, Ectors N, Declercq J, Creemers JW. Phlorizin pretreatment reduces acute renal toxicity in a mouse model for diabetic nephropathy. J Biol Chem. 2013; 288:27200–27207. [PubMed: 23940028]
47. Jin X, Zeng L, He S, Chen Y, Tian B, Mai G, Yang G, Wei L, Zhang Y, Li H, Wang L, Qiao C, Cheng J, Lu Y. Comparison of single high-dose streptozotocin with partial pancreatectomy combined with low-dose streptozotocin for diabetes induction in rhesus monkeys. Exp Biol Med (Maywood). 2010; 235:877–885. [PubMed: 20558842]
48. Loeffler I, Liebisch M, Wolf G. Collagen VIII influences epithelial phenotypic changes in experimental diabetic nephropathy. Am J Physiol Renal Physiol. 2012; 303:F733–F745. [PubMed: 22759394]
49. Noonan WT, Banks RO. Renal function and glucose transport in male and female mice with diet-induced type II diabetes mellitus. Proc Soc Exp Biol Med. 2000; 225:221–230. [PubMed: 11082217]
50. Hartner A, Cordasic N, Klanke B, Veelken R, Hilgers KF. Strain differences in the development of hypertension and glomerular lesions induced by deoxycorticosterone acetate salt in mice. Nephrol Dial Transplant. 2003; 18:1999–2004. [PubMed: 13679473]

Highlights

1. First time to show that C66 prevents DN via epigenetic mechanism.
2. First time to show that C66 prevents DN via inactivation of JNK-mediated epigenetic modification.
3. First to show that C66 treatment can provide a sustained prevention of DN.
4. C66 is stronger curcumin analogue, with high effectiveness at low dose range.

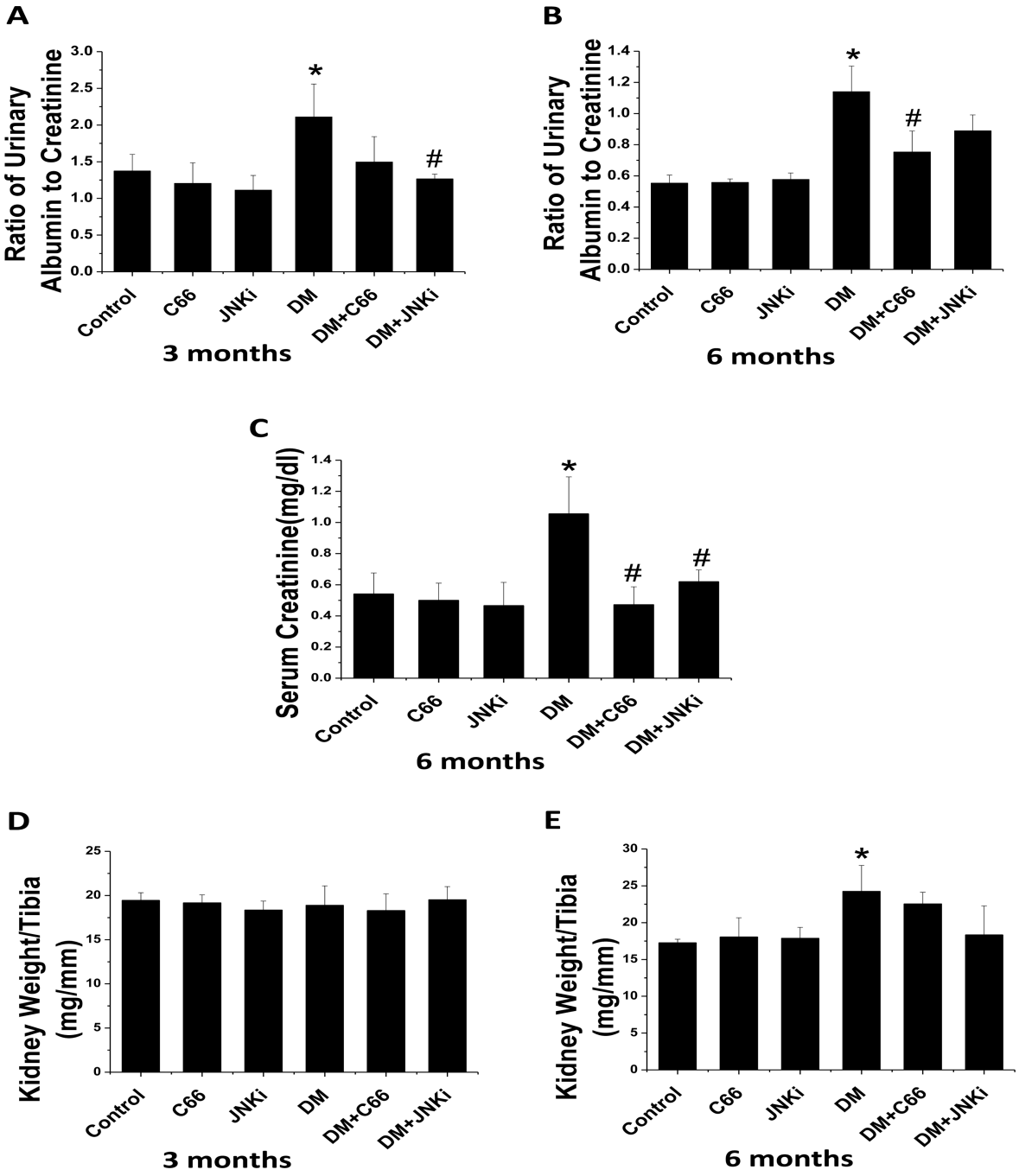

Figure 1. C66 prevented diabetes-induced renal functional changes

Spot urine and serum samples were collected from mice and the urinary albumin-to-creatinine ratio were determined after (A) 3 months of treatment and (B) 6 months after treatment (equating to 3 months after treatment termination). The serum creatinine levels (C) were examined at the 6-month period to determine renal function. Kidney weight was normalized to tibia length (D, 3 months; E, 6 months). Data are presented as mean ± SD after normalizing to control (n≥4). * $P < 0.05$ vs. control group; # $P < 0.05$ vs. DM group.

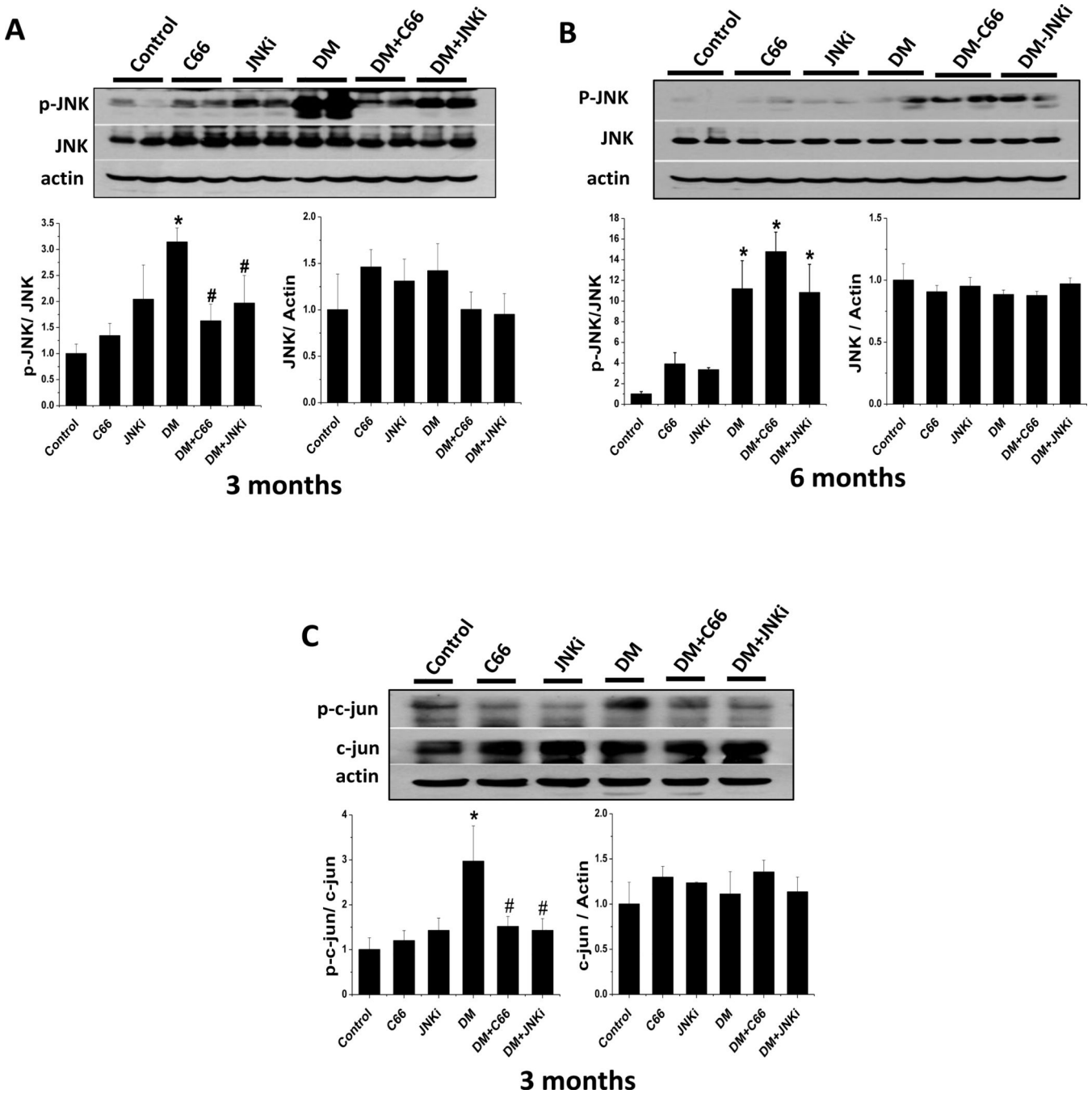

Figure 2. C66 down-regulated diabetes-induced renal JNK pathway activity

Western blotting assay was performed to measure the expressions of phosphorylated-JNK and total JNK after (A) 3 months of treatment and (B) 6 months after treatment (equating to 3 months after treatment termination). The downstream proteins, phoso-c-jun (p-c-jun) and c-jun, were also measured at the 3-month time-point (C). The sample in each lane represents total proteins collected from each individual animal, and the data are presented as mean ± SD after normalizing to control (n≥4). * $P < 0.05$ vs. control group; # $P < 0.05$ vs. DM group.

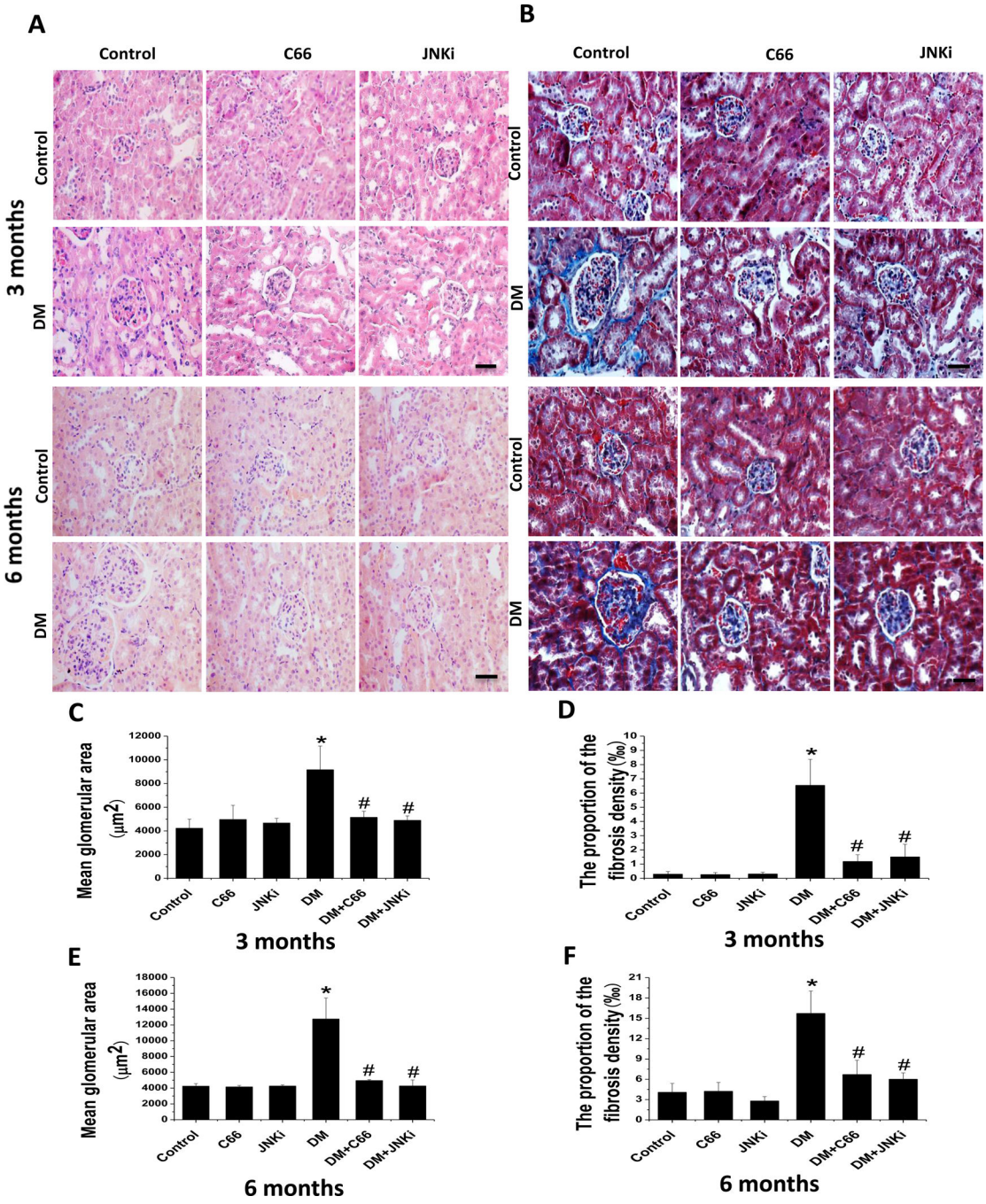

Figure 3. C66 prevented diabetes-induced renal structural changes

(A) Renal pathology shown by H&E staining. (B) Renal fibrosis shown by Masson's Trichrome staining. Glomerular enlargement at (C, D) 3 months of treatment and (E, F) 6 months after treatment (equating to 3 months after treatment termination) was quantitated by calculating (C, E) the mean glomerular area and (D, F) the percentage of the area with positivity for Masson's staining. Original magnification: ×200. Bar: 50 μm.

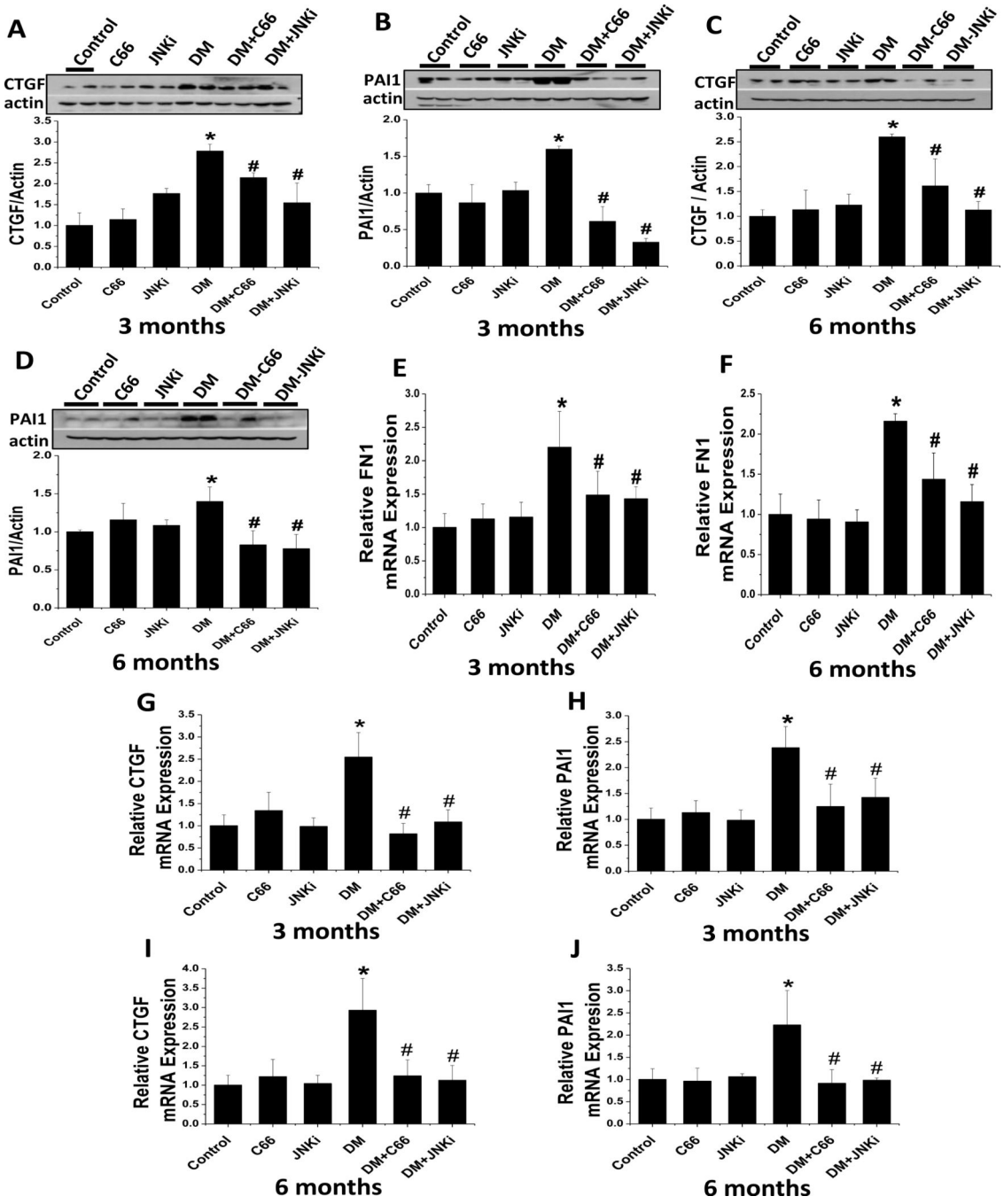

Figure 4. C66 prevented diabetes-induced renal fibrosis

Western blotting assay was used to measure the protein expression levels of the fibrosis-related cytokines (A, C) CTGF and (B, D) PAI-1 in kidneys of mice at (A, B) 3 months of treatment and (C, D) 6 months after treatment (equating to 3 months after treatment termination). Representative samples from one mouse in each group are shown. Real-time PCR was used to measure the mRNA expression levels of (E, F) fibronectin 1 (FN-1), (G, I) CTGF and (H, J) PAI-1, relative to GAPDH, at (E, G, H) 3 months of treatment and (F, I, J) 6 months after treatment (equating to 3 months after treatment termination). Data are

presented as mean ± SD after normalizing to control (n≥4). * $P < 0.05$ vs. control group; $^{\#}$ $P < 0.05$ vs. DM group.

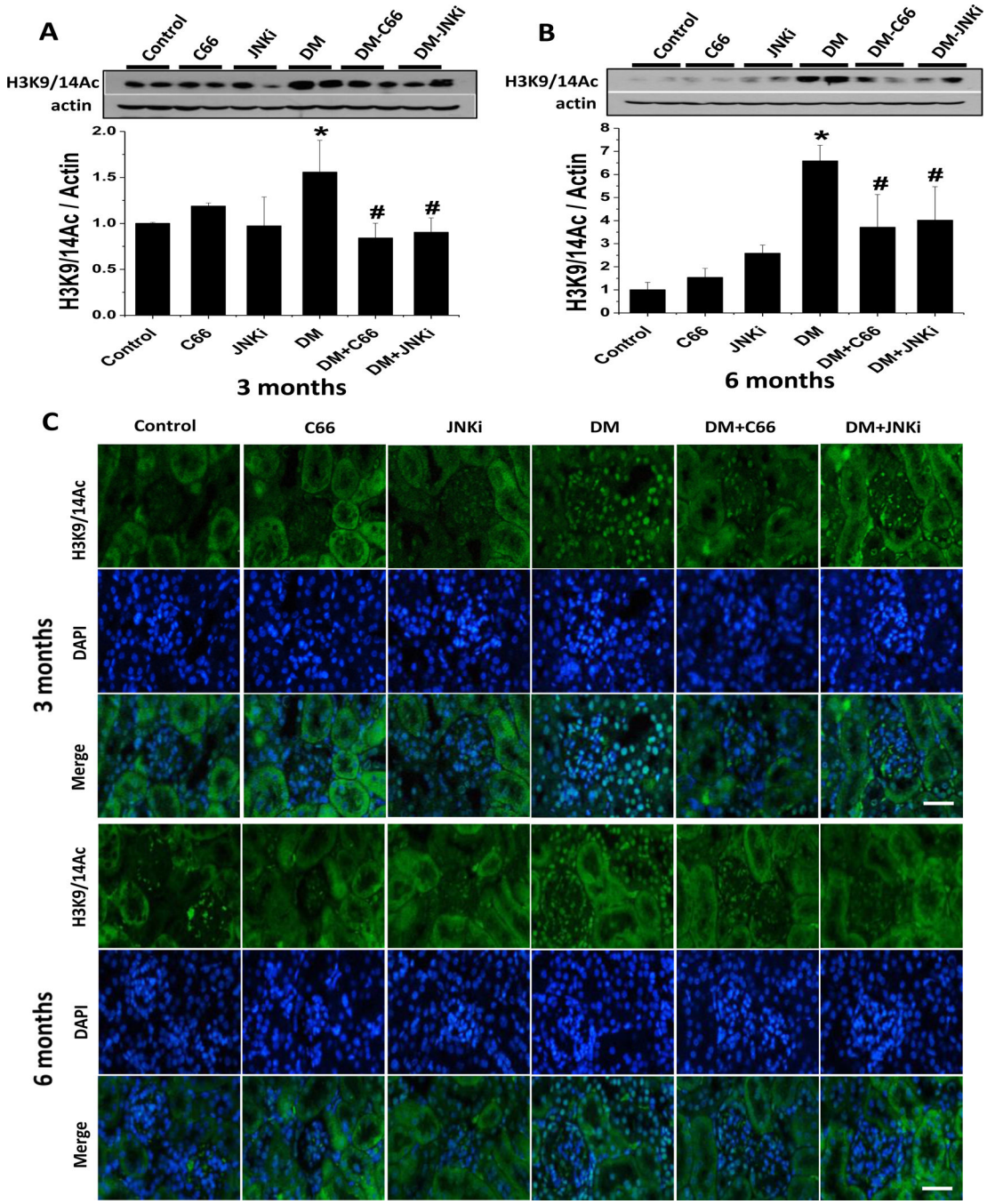

Figure 5. C66 prevented diabetes-induced renal histone acetylation

Expression of renal H3K9/14 was measured by (A, B) western blotting assay and (C) immunofluorescence staining at (A, C) 3 months of treatment and (B, C) 6 months after treatment (equating to 3 months after treatment termination). In panel C, H3K9/14 is shown as present (green fluorescence) in the nuclei (blue fluorescence; DAPI staining) of both glomerular cells and renal tubular cells; original magnification: ×200. Data are presented as mean ± SD after normalizing to control (n≥4). * $P < 0.05$ vs. control group; # $P < 0.05$ vs. DM group. Bar: 50 μm.

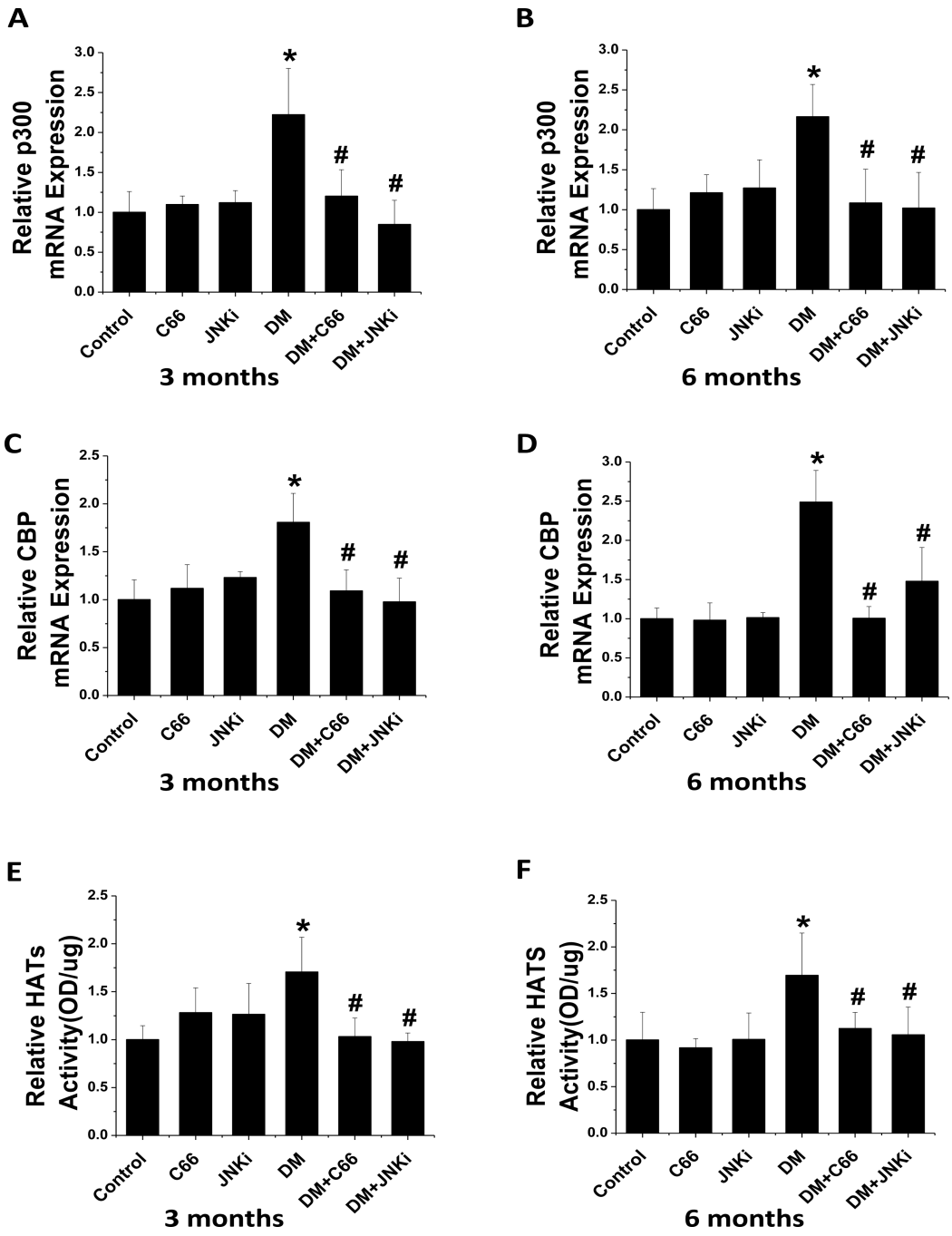

Figure 6. C66 down-regulated diabetes-induced renal expression of the p300/CBP HATs and HATs' activity

Real-time PCR was used to measure the mRNA expression of (A, B) p300 and (C, D) CBP, relative to GAPDH, at (A, C) 3 months of treatment and (B, C) 6 months after treatment (equating to 3 months after treatment termination). Fraction was used to indicate the HATs activity, relative to control at (E) 3 months of treatment and (F) 6 months after treatment (equating to 3 months after treatment termination). Data are presented as mean ± SD after normalizing to control (n≥4). * $P < 0.05$ vs. control group; $^{\#}$ $P < 0.05$ vs. DM group.

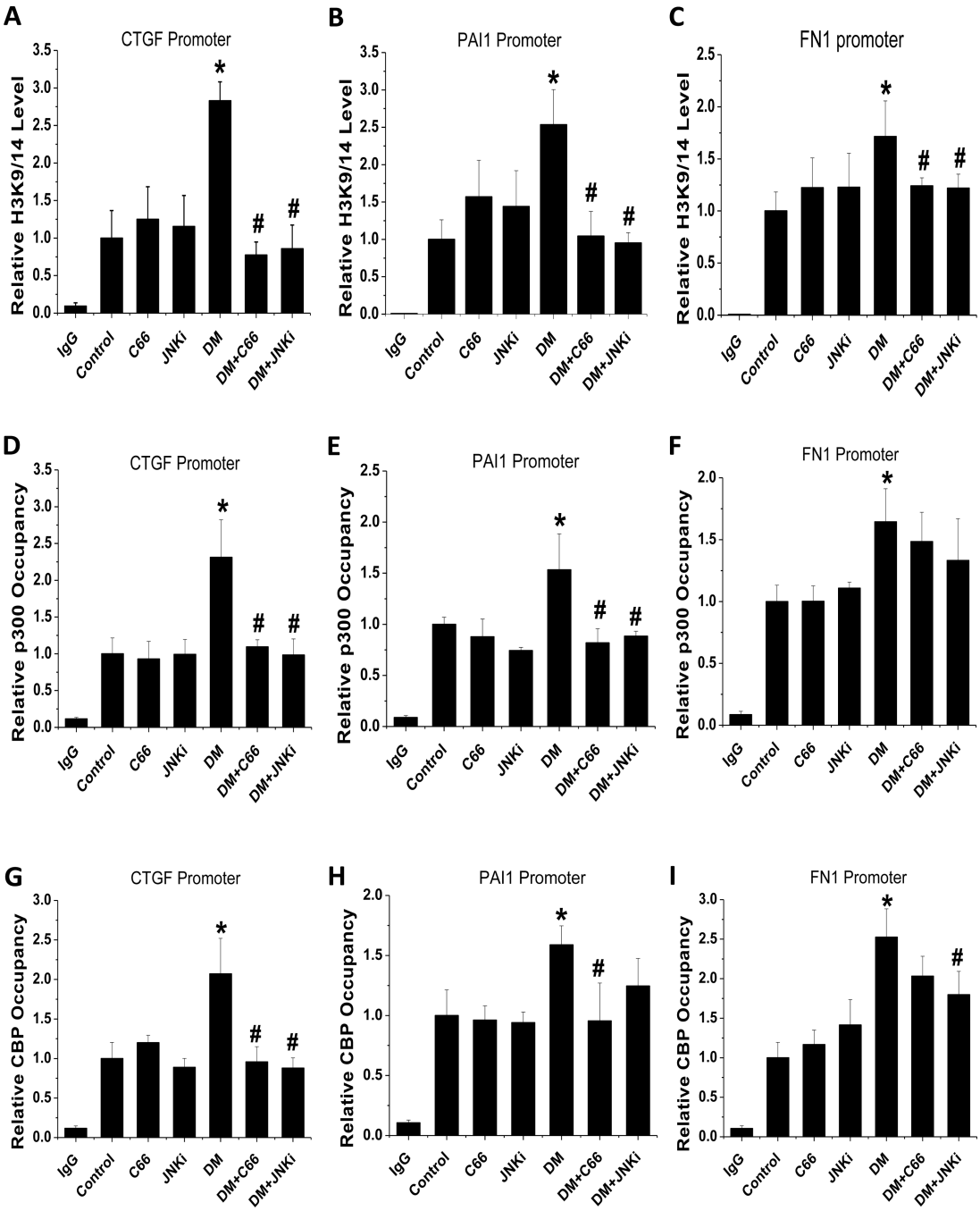

Figure 7. C66 produced a persistent decrease in the diabetes-induced increase in renal H3K9/14 levels on the promoters of CTGF, PAI-1 and FN-1 genes

CHIP assay was used to detect the (A, B, C) H3K9/14 levels and (D, E, F) p300 occupancy on the (A) CTGF, (B) PAI-1 and (C) FN-1 promoters at 6 months after treatment (equating to 3 months after treatment termination). Normal mouse IgG was used as a negative control and data were normalized to input DNA samples. n=5; * $P < 0.05$ vs. control group; # $P < 0.05$ vs. DM group.

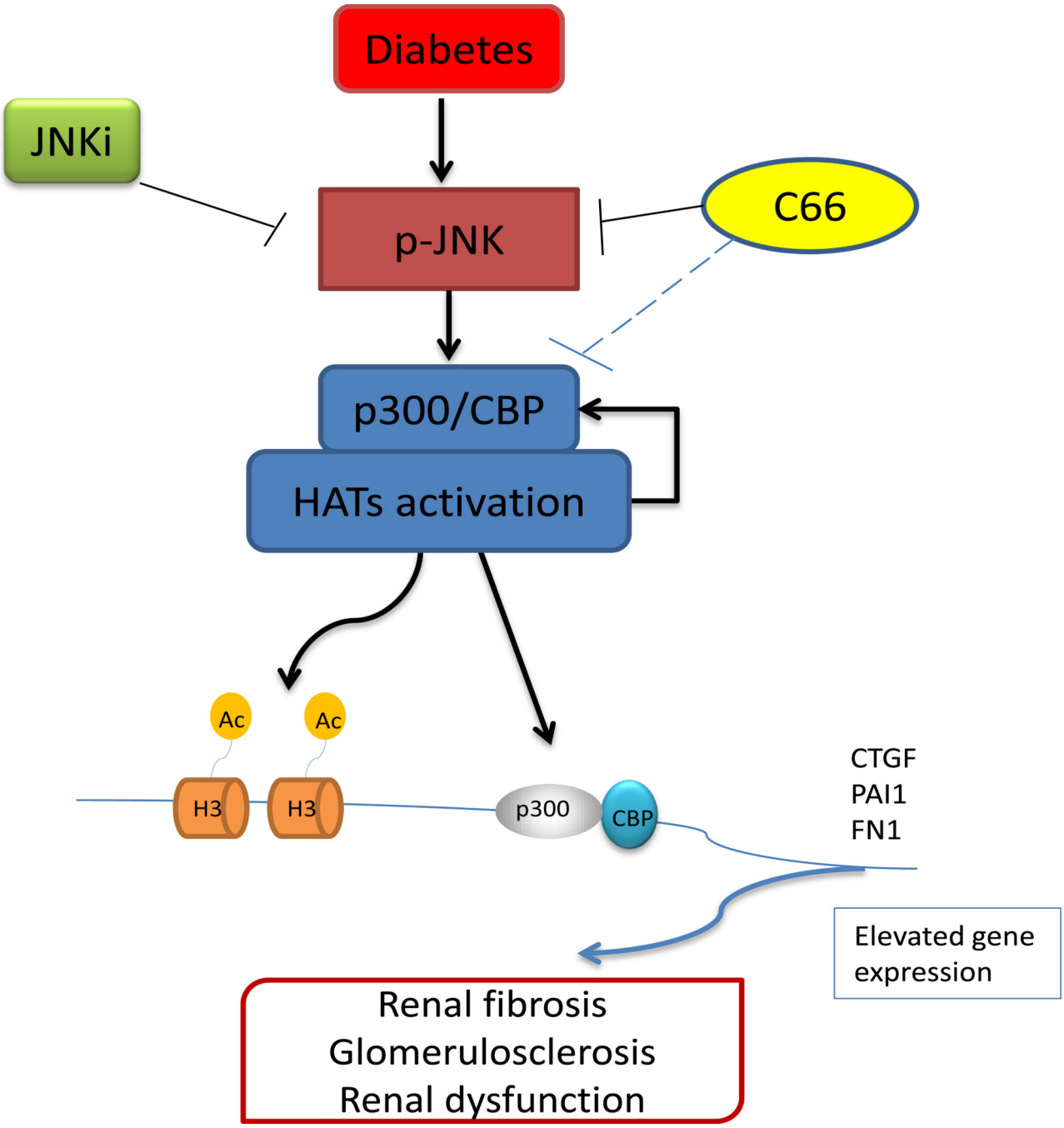

Figure 8. Schematic illustration of the protective mechanism of C66 against diabetes-induced renal fibrosis and progression of DN

The mechanism involves inhibition of activation of the JNK pathway via epigenetic modulation of p300/CBP-mediated histone acetylation. In the kidneys of the STZ-induced diabetic mouse model, the JNK-induced activation of p300/CBP HATs promotes histone lysine acetylation at target gene promoters, such as CTGF, PAI-1 and FN-1, as well as the occupancy of p300/CBP on the promoters of these genes. These events can enhance the expression of CTGF, PAI-1 and FN-1 genes, resulting in renal fibrosis and glomerulosclerosis, both of which are involved in DN pathogenesis. C66 can prevent these

changes though its effects on the JNK pathway and histone acetylation. Curcumin, for which C66 analogue is the analogue, is an inhibitor of p300/CBP, but whether curcumin can inhibit the p300/CBP complex's expression, activation or function remains unknown.